Localization of Unconventional Myosins V and VI in Neuronal Growth Cones

Daniel M. Suter,[1] Foued S. Espindola,[1,4,*] Chi-Hung Lin,[1,†] Paul Forscher,[1] Mark S. Mooseker[1,2,3]

[1] Department of Molecular, Cellular, and Developmental Biology, Yale University, New Haven, Connecticut 06520

[2] Department of Cell Biology, Yale University, New Haven, Connecticut 06520

[3] Department of Pathology, Yale University, New Haven, Connecticut 06520

[4] Departments of Genetics and Biochemistry, University Federal of Uberlandia, Uberlandia, MG 38400-982, Brazil

Received 20 August 1999; accepted 27 September 1999

ABSTRACT: **Class V and VI myosins, two of the six known classes of actin-based motor genes expressed in vertebrate brain (Class I, II, V, VI, IX, and XV), have been suggested to be organelle motors. In this report, the neuronal expression and subcellular localization of chicken brain myosin V and myosin VI is examined. Both myosins are expressed in brain during embryogenesis. In cultured dorsal root ganglion (DRG) neurons, immunolocalization of myosin V and myosin VI revealed a similar distribution for these two myosins. Both are present within cell bodies, neurites and growth cones. Both of these myosins exhibit punctate labeling patterns that are found in the same subcellular region as microtubules in growth cone central domains. In peripheral growth cone domains, where individual puncta are more readily resolved, we observe a similar number of myosin V and myosin VI puncta. However, less than 20% of myosin V and myosin VI puncta colocalize with each other in the peripheral domains. After live cell extraction, punctate staining of myosin V and myosin VI is reduced in peripheral domains. However, we do not detect such changes in the central domains, suggesting that these myosins are associated with cytoskeletal/organelle structures. In peripheral growth cone domains myosin VI exhibits a higher extractability than myosin V. This difference between myosin V and VI was also found in a biochemical growth cone particle preparation from brain, suggesting that a significant portion of these two motors has a distinct subcellular distribution.** © 2000 John Wiley & Sons, Inc. J Neurobiol 42: 370–382, 2000

Keywords: **myosin V; myosin VI; neuronal growth cone; dorsal root ganglia neurons; cytoskeleton; subcellular localization**

The myosin superfamily consists of at least 15 structurally distinct classes of actin-based molecular motors (Mermall et al., 1998; Probst et al., 1998; Wang et al., 1998). In addition to the well-defined roles of conventional or class II myosins in mediating actin-based contractile phenomena in muscle and non-muscle cells, a wide range of functions have been proposed for various "unconventional" members of

Correspondence to: D. M. Suter (daniel.suter@yale.edu).

* *Present address:* Department of Genetics and Biochemistry, University Federal of Uberlandia, Uberlandia, MG 38400-982, Brazil

† *Present address:* Institute of Microbiology and Immunology, National Yang-Ming University, Taipei, Taiwan

Contract grant sponsor: MDA (M.S.M.).

Contract grant sponsor: National Institutes of Health; contract grant number: DK-25387 and PPG 1-P01-DK55389-01 (M.S.M.) and NS-28695 (P.F.).

Contract grant sponsor: Swiss National Science Foundation (D.M.S.).

Contract grant sponsor: Pew Charitable Trust—Latin American Fellows Program (F.S.E.).

Contract grant sponsor: Conselho Nacional de Desenvolvimento Cientifico e Tecnologico (F.S.E.).

this gene family. Based largely on genetic and molecular genetic evidence, these functions include organelle movement, endo- and exocytosis, transport of mRNA, signal transduction, and mechanoregulation of ion channels (Mermall et al., 1998). In vertebrates, at least eight (I, II, V, VI, VII, IX, X, XV) of these classes (most of which have multiple members) are expressed. In the vertebrate nervous system, representatives of most of these myosin classes have been identified (reviewed in Hasson and Mooseker, 1997). In this study we focus on the neuronal expression of two myosins of these classes, V and VI, whose members have been implicated in actin-based organelle transport in a variety of systems (Mermall et al., 1998).

There are three known class V myosin heavy chain genes expressed in vertebrates (Mercer et al., 1991; Espreafico et al., 1992; Bement et al., 1994; Hasson et al., 1996; Zhao et al., 1996; Rodriguez and Cheney, abstract, Mol Biol Cell 1998, 9, 20a) only one of which, brain myosin V, has been extensively characterized both genetically and biochemically (reviewed in Mooseker and Cheney, 1995; Titus, 1997). Like other known myosins, the myosin V heavy chain consists of an amino-terminal motor or head domain, a neck or regulatory domain consisting of six IQ motifs, each a site for light chain binding, and a C-terminal tail consisting of a proximal "stalk" domain comprised of coiled-coil forming alpha helical segments, followed by distal globular domain. The subunit composition of myosin V is the most complex of known myosins; it consists of two heavy chains, each of which has several neck-associated light chains, ~5 of which are calmodulin, one of which is an essential light chain also present in brain myosin II, and a tail-associated light chain that is also a subunit of dynein (Espindola et al., abstract, Mol Biol Cell 1996, 7, 372a; Benashski et al., 1997). Very recently, myosin V has also been shown to bind and activate CaM-kinase II, probably by delivering calmodulin to the kinase (Costa et al., 1999). *In vitro* assays revealed that purified myosin V is a Ca^{2+}-regulated, barbed end–directed motor (Cheney et al., 1993) that binds F-actin with high affinity in the presence of ATP (Nascimento et al., 1996).

There is now broad biochemical, cytological, and genetic evidence that myosin V may be an important organelle motor (for reviews, see Titus, 1997; Mermall et al., 1998). For example, it has been demonstrated that myosin V associates with small organelles in growth cones of rat superior cervical ganglion neurons (Evans et al., 1997) and that myosin V can act as an actin-based vesicle motor (Evans et al., 1998; Tabb et al., 1998). Analysis of myosin V in *dilute* mice, which carry mutations in the myosin V gene (Mercer et al., 1991), provide further evidence that this motor is involved in organelle movement in Purkinje cells (Takagishi et al., 1996) and melanocytes (Provance et al., 1996; Nascimento et al., 1997; Wu et al., 1997; Rogers and Gelfand, 1998; Wu et al., 1998).

In contrast to myosin V, myosin VI is less well characterized, especially with respect to its biochemical properties, expression pattern, and potential roles in actin-based motility. The myosin VI heavy chain is a 140-kDa protein with a typical amino-terminal head domain containing actin- and ATP-binding activity, a short neck with one IQ motif, and a relatively short tail domain with a coiled-coil region (Kellerman and Miller, 1992; Hasson and Mooseker, 1994; Avraham et al., 1995, 1997; Buss et al., 1998). Interestingly, it was found that a mutation of myosin VI gene is responsible for the *Snell's waltzer* phenotype in mouse, a form of severe hearing loss and vestibular dysfunction (Avraham et al., 1995). Immunofluorescence studies of myosin VI in the inner ear revealed that this unconventional myosin is concentrated in the cuticular plate of the hair cells, suggesting that myosin VI may have a role in attachment of stereocilia rootlets to the cuticular plate (Hasson et al., 1997).

Besides this more static function for myosin VI, there is also evidence for involvement of this motor in organelle transport, since myosin VI was localized in the pericuticular necklace, a vesicle-rich compartment of inner ear hair cells (Hasson et al., 1997). Furthermore, functional and localization studies in the *Drosophila* embryo suggest a role for myosin VI as a transport motor for cytoplasmic particles (Mermall et al., 1994; Mermall and Miller, 1995; Bohrmann, 1997; Lantz and Miller, 1998). Myosin VI has also been shown to interact with a glucose transporter binding protein GLUT1CBP, which was implicated as a linker between the motor protein and transporter carrying vesicles (Bunn et al., 1999). Finally, a recent report has provided evidence that myosin VI may have a function in membrane ruffling and membrane traffic pathways in fibroblasts (Buss et al., 1998).

To gain more insights into the neuronal functions of myosin V and myosin VI, we investigated their distribution in cultured chick dorsal root ganglion (DRG) neurons, focusing on their localization in the growth cone. Our immunolocalization experiments revealed a punctate staining pattern in the growth cone for both myosins, partially colocalizing with each other. Despite these similarities, localization and fractionation data suggest that a significant fraction of these two motors have a distinct subcellular distribution in growth cones.

MATERIALS AND METHODS

Antibodies

The following affinity-purified antibodies to myosin V and myosin VI were used in this study: rabbit anti-myosin V-tail; rabbit anti-myosin V-head (both described in Espreafico et al., 1992); rat anti-myosin V-head; rabbit anti-myosin VI-tail (Hasson and Mooseker, 1994). Monoclonal antibodies to β-tubulin and GAP-43 (clone GAP-7B10) were purchased from Sigma Chemical Co. (St. Louis, MO).

Western Blot Analysis of Myosin V and Myosin VI Expression

Chick embryos at different stages throughout embryonic development were used for analysis of myosin V and myosin VI expression in DRG and total brain: stage 29 [embryonic day 6 (E6)], 33 (E8), 36 (E10), 38 (E12), 42–43 (E16), and 45 (E19). Total brain and DRGs were washed with phosphate-buffered saline (PBS) containing 1 m*M* Pefabloc (Boehringer Mannheim, Indianapolis, IN) and homogenized in 5% cold trichloroacetic acid (TCA). After a spin at 14,000 $\times$ *g* for 10 min, the pellets were first resuspended with 100 m*M* Tris-HCl, pH 8.8, and then were boiled in sample buffer. Equal protein amounts were separated on a 4–20% polyacrylamide gel. Proteins were transferred onto nitrocellulose and probed with rabbit anti-myosin V-tail, rabbit anti-myosin V-head, and rabbit anti-myosin VI-tail antibodies. Detection was carried out with the ECL method according to the manufacturer's instructions (Boehringer Mannheim).

Cell Culture

Dissociated DRG neurons from 10-day-old chicken embryos were cultured on laminin-coated coverslips in Dulbecco's modified Eagle's medium-F12, 5% horse serum, 2% chicken serum (all from Life Technologies, Frederick, MD), 14 m*M* $NaHCO_3$, 15 m*M* Hepes, pH 7.4, penicillin-streptomycin-fungizone 1:100 (JRH Bioscience, Lenexa, KS), and 20 ng/mL NGF. Coverslips were acid- and ethanol-washed and precoated with 20 μg/mL poly-L-lysine in H_2O for 30 min at room temperature (RT). After three washes with H_2O, poly-lysine–coated coverslips were air-dried and stored until they were used for culturing cells. Prior to plating dissociated DRG neurons, the coverslips were coated with 80 μL of 20 μg/mL laminin (Life Technologies) in PBS for 2 h in a humidified 37°C incubator followed by two PBS washing steps. DRGs were collected into ice-cold Puck's saline and dissociated by trypsin treatment and trituration using a Pasteur pipette. About 15,000 DRG cells were plated per coverslip in the medium described above and typically were maintained for 16–20 h in a humidified 37°C incubator (5% CO_2) before use.

Immunocytochemical Stainings

After a 16 h incubation at 37°C, the cells were fixed with warm fixation buffer: 4% paraformaldehyde in 60 m*M* PIPES, 25 m*M* HEPES, pH 7, 5 m*M* EGTA, 3% sucrose (PHEM buffer) for 1 h at RT. After three washes with PBS, the cells were permeabilized with 0.1% Triton X-100 in PBS for 10 min at RT. Following additional PBS washing and blocking with 5% bovine serum albumin (Sigma), 10% normal goat serum, 0.5% gelatin (Sigma) in PBS for 30 min, the cells were incubated with primary antibodies in 1:5 blocking solution/PBS for 1 h at 37°C. All myosin V and myosin VI antibodies were used at 5–10 μg/mL. The monoclonal mouse anti-β-tubulin antibody (Sigma) was incubated at 1:200. After washing with PBS, secondary antibody incubation was at 1:200 for 30 min at RT. Secondary Texas Red- or FITC-labeled donkey antibodies were purchased either from Amersham (Princeton, NJ) or Jackson ImmunoResearch (West Grove, PA). For visualization of F-actin structures, rhodamine-phalloidin (Molecular Probes, Eugene, OR) was used at 1:100. Coverslips were mounted on glass slides using Citifluor (Citifluor Products, Canterbury, UK) as an antifading agent. The cells were inspected on an inverted microscope (Nikon, Melville, NY) using a 100$\times$/1.3 NA objective. Images were acquired with a cooled CCD camera (Image Point, Photometrics, Tucson, AZ) controlled by Metamorph software (Universal Imaging Corporation, West Chester, PA). Image processing was carried out in Adobe Photoshop 4.0 (Adobe Systems Incorporated, San Jose, CA). For quantification of puncta, we analyzed color overlays of myosin V and VI double stainings, using the manual count object tool of Metamorph. Single- and double-labeled puncta were counted only in the peripheral growth cone domain where individual puncta could be more readily resolved. Average values $\pm$ S.E.M. are given; Student's *t*-tests were performed to analyze differences between data sets.

Live Cell Extraction

For live cell extraction experiments, DRG cell cultures were treated with 0.02% of saponin in PHEM buffer for 30 s immediately followed by fixation with 4% paraformaldehyde in PHEM buffer containing 1% Triton X-100 for 10 min. The fixation process was completed using the fixation solution described above in the absence of any detergent for 50 min. To investigate structural changes during the live cell extraction process, the cells were observed using high-resolution, video-enhanced differential interference contrast (DIC) microscopy. Therefore, the cells were mounted into a custom-made chamber, kept at 34°C, and inspected on Zeiss Axiovert-10 microscope (Zeiss, Thornwood, NY) using a 63$\times$/1.4 NA oil immersion objective. Image acquisition and processing were carried out as recently described (Suter et al., 1998).

Subcellular Fractionation with Differential Centrifugation

Total brains from 2 chick embryos (E10) were homogenized with the same buffer used for the live cell extraction experiment (PHEM, 0.02% saponin) containing 0.2 m*M* dithiothreitol (DTT), 1 m*M* Pefabloc, and 5 μg/mL leupeptin (Sigma). Cell lysis was verified by light microscopy. The low-speed spin was carried out at 1000 $\times$ *g* for 20 min, the high-speed spin at 30,000 $\times$ *g* for 20 min, and the ultra-speed spin at 120,000 $\times$ *g* for 2.5 h. Protein determination was done according to the BCA-method (Pierce Chemical Co., Rockford, IL). Stochiometric amounts of each fraction were separated on a 5–20% SDS-PAGE and blotted to nitrocellulose membrane. Blots were probed with rabbit anti-myosin V-tail and anti-myosin VI-tail antibodies at 0.5 μg/mL each. Detection was carried out with the ECL method according to the manufacturer's instructions (Boehringer Mannheim). Metamorph software (Universal Imaging Corporation) was used for blot quantification.

Growth Cone Particle Preparation

Growth cone particles were isolated as modified from Pfenninger et al. (1983) and Lohse et al. (1996). All steps were carried out at 4°C. The total brains of 9 chicken embryos (E10) were homogenized with 20 strokes in a Dounce homogenizer using 6 volumes of the following buffer: 0.32 *M* sucrose, 10 m*M* HEPES, pH 7.3, 5 m*M* EGTA, 0.2 m*M* DTT, 1 m*M* Pefabloc, 10 μg/mL leupeptin (Sigma), 10 μg/mL pepstatin A (Sigma), and 10 μg/mL aprotinin (Sigma). Cell lysis was verified by light microscopy. The homogenate was spun at 1400 $\times$ *g* for 15 min. The supernatant of this low-speed spin was loaded onto 0.83 *M* sucrose in the same buffer as above and spun at 150,000 $\times$ *g* for 1 h. The interface material containing growth cone particles was collected with a long needle, diluted with 3 volumes of homogenization buffer, and spun at 40,000 $\times$ *g* for 30 min. The resulting pellet represents the growth cone particle and was resuspended in homogenization buffer for western blot analysis. A corresponding pellet containing growth cone particles was further extracted with 0.2% saponin in homogenization buffer for 30 min and spun at 150,000 $\times$ *g* for 2 h to separate extracted proteins from growth cone particles. From each fractionation step samples were collected for determination of protein concentration and western blotting (pellet fractions were resuspended to the original sample volume). Protein determination was done according to the BCA method (Pierce Chemical Co.). Equal protein amounts (15 μg) from each fraction were separated on 5–20% SDS-PAGE and processed for western blotting as described above. As control for the growth cone particle isolation, we used a monoclonal antibody against GAP-43 (clone GAP-7B10; Sigma) at 3 μg/mL.

RESULTS

Myosin V and Myosin VI Are Expressed in the Chick Nervous System during Embryonic Development

To investigate the expression pattern of myosin V and myosin VI in the developing chick central and peripheral nervous system, we carried out Western blot analysis of whole brain and DRG extracts at different stages of embryonic development (Fig. 1). Using affinity-purified antibodies to myosin V and myosin VI, both unconventional myosins were detected in chicken brain between embryonic days 6 and 14, respectively [Fig. 1(B)]. The presence of the myosin VI heavy chain was revealed with a rabbit antibody to the tail of myosin VI, whereas the myosin V heavy chain was detected by two distinct rabbit antibodies to the tail and head of myosin V. The level of myosin VI expression in the brain remains constant between E6 and E14. In contrast, brain myosin V expression increases during this time period. In DRGs, we found an increase in both myosin V and VI expression at stage E10, a time period in development when the DRGs increase in size [Fig. 1(B)]. To summarize, both myosins are expressed in the chick central and peripheral nervous system in a similar pattern during embryonic development.

Myosin V and Myosin VI Are Expressed in Cultured Chick DRG Neurons

Dissociated chick DRG neurons of E10 were cultivated on laminin substrata for immunolocalization of myosin V and myosin VI. Both myosin V and myosin VI were detected in neuronal cell bodies, neurites, and growth cones [Fig. 2(A,B)]. DRG neurons exhibit a variety of growth cone morphologies on laminin substrata: from fanlike growth cones [Fig. 2(C)] to the ones with large filopodia but small lamellipodia [Fig. 3(A)]. One can distinguish between two major cytoplasmic domains in neuronal growth cones: the central, microtubule-rich domain and the peripheral, F-actin–rich domain [Forscher and Smith, 1988; see Fig. 2(D)]. In general, both myosins exhibit a punctate staining pattern in growth cones, with a higher concentration of puncta in the central domain compared to the peripheral domain [Fig. 2(C,D)]. Double stainings revealed that 17 $\pm$ 2% of the myosin V and 18 $\pm$ 3% of the myosin VI puncta in the peripheral domain colocalize with each other [Fig. 4(L); for quantification see Fig. 5(A)]. In the central domain, the degree of myosin V and VI puncta colocalization is difficult to estimate, because the puncta are densely

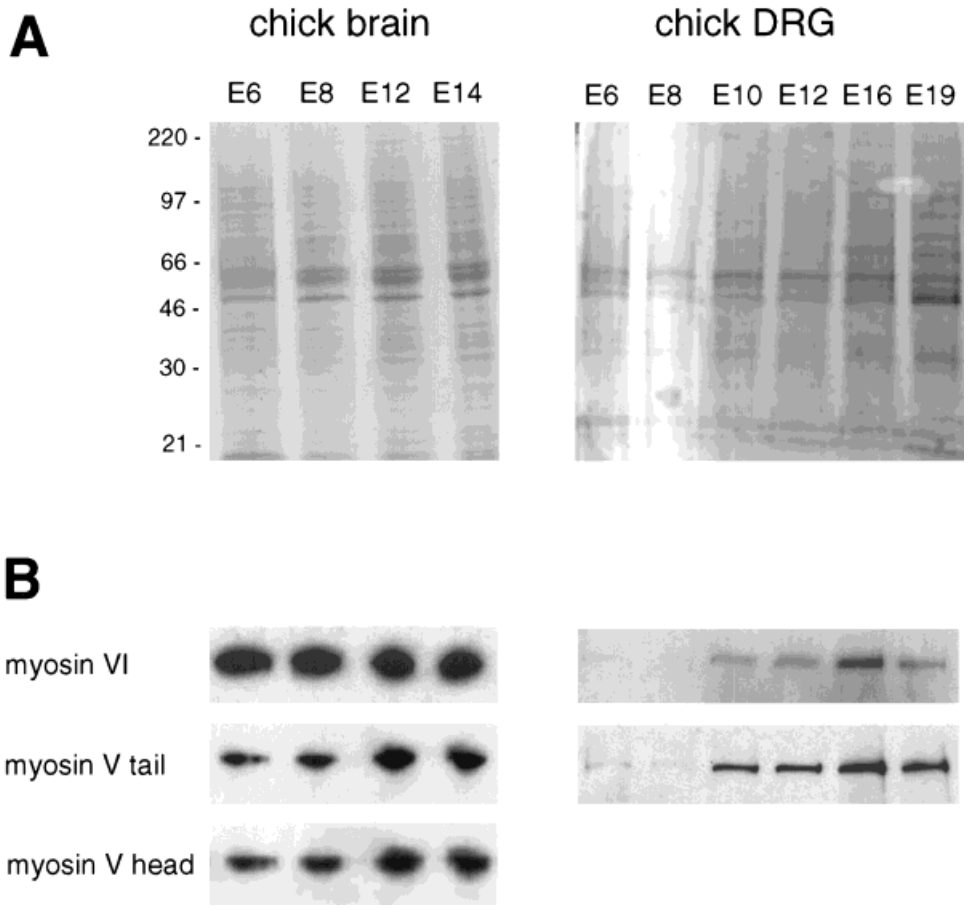

Figure 1 Myosin V and myosin VI are expressed in brain and DRGs of developing chick embryos. Whole brain and DRGs of chick embryos [embryonic day (E)6 to E19] were homogenized in 5% TCA and equal amounts of protein (10 μg) were separated on 4–20% SDS-PAGE. (A) Total protein visualized by Coomassie Blue stain. (B) The respective Western blots were probed with affinity-purified rabbit anti-myosin V tail and head antibodies, and rabbit anti-myosin VI tail antibody, respectively.

packed in this region that is thicker that the peripheral domain [Fig. 4(L)]. When myosin V and VI were detected with the same secondary antibody on different cultures, the stainings had similar intensities, myosin V appearing somewhat more abundant (data not shown). The punctate distribution of myosin V and myosin VI suggests that these myosins might be associated with organelle structures in the growth cone, although this may not be true for all puncta, as found in other myosin localization studies (Lewis and Bridgman, 1996; Evans et al., 1997). However, in some growth cones (Fig. 3) we observe that a fraction of these myosins (especially of myosin VI) can exhibit a more diffuse staining pattern, suggesting a cytosolic protein fraction.

Further analysis of the myosin V and myosin VI distribution in growth cones was carried out with respect to the major cytoskeletal structures, F-actin and microtubules (Fig. 3). Both myosins are found in the same subcellular region as microtubules in the central domain [Fig. 3(C,D) and (G,H)]. In the peripheral domain, myosin V is present in F-actin–containing lamellipodia and filopodia [Fig. 3(A,B)], whereas myosin VI shows very little overlap with F-actin structures [Fig. 3(E,F)].

Subcellular Association of Myosin V and Myosin VI in Growth Cones

We further investigated the subcellular association state of myosin V and myosin VI in growth cones by three different types of experiments: (1) live cell extraction, (2) nocodazole treatment of cultured DRG neurons, and (3) Western blot analysis of growth cone particle preparations.

Live cell extraction experiments should help to

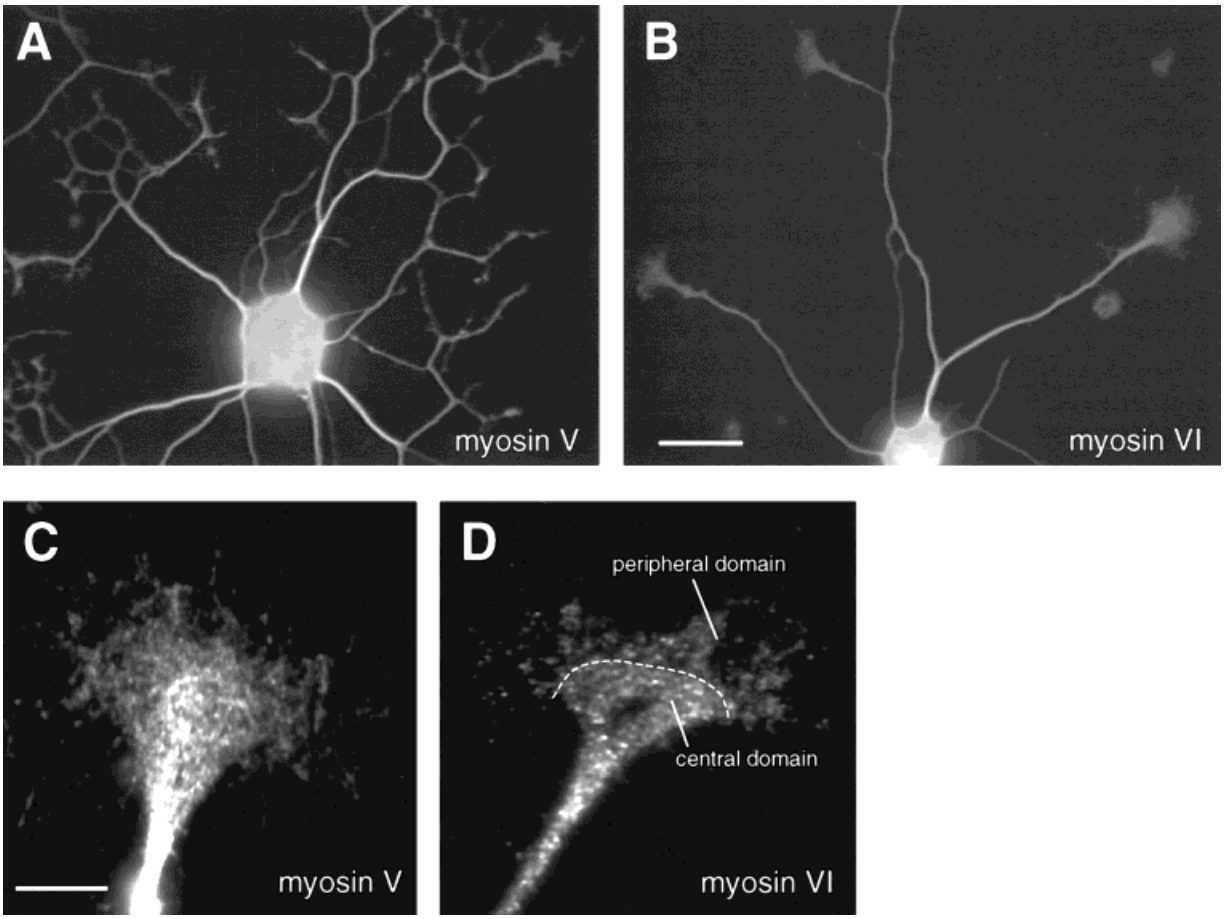

Figure 2 Expression of myosin V and myosin VI in cultured DRG neurons. DRG neurons cultured on laminin substrata were fixed after 20 h and immunostained for myosin V (A, C) and myosin VI (B, D). Both myosin V (A) and myosin VI (B) are localized in the neuronal cell body, neurites, and growth cones. A more detailed view of myosin V and myosin VI distributions in the growth cone are shown in (C) and (D). Both myosin V and myosin VI exhibit a punctate distribution with its highest concentration in the central domain of the growth cone. Bars: (A, B) 25 μm; (C, D) 5 μm.

determine whether there is a significant fraction of readily extractable, presumably cytosolic, myosin V or myosin VI [Fig. 4(A–K)]. DRG neurons were treated for 30 s with 0.02% saponin followed by fixation in the presence of 1% Triton X-100 (see Materials and Methods). Figure 4(A–C) shows the structural changes during such an experimental treatment visualized by high-resolution DIC video microscopy. Saponin, which disrupts the plasma membrane, causes a "fuzzy" appearance of the growth cone cell surface when observed in DIC [Fig. 4(B)]. This "fuzzy" look of the growth cone disappeared after further removal of membranes by Triton X-100 during the fixation process [Fig. 4(C)].

Purely cytosolic proteins should not be detected in significant amounts by immunocytochemistry using an extraction procedure as described above. In contrast, nonextractable protein complexes such as microtubules and F-actin should not be affected by this treatment. Indeed, microtubule and F-actin staining [Fig. 4(D,F)] were indistinguishable from control stainings during which cells were extracted after fixation [Fig. 3(A,C,E,G)]. Interestingly, the staining pattern of myosin V and myosin VI after live cell extraction [Fig. 4(E,G,H,I,K)] was similar to the control condition [Fig. 2(C,D), Fig. 4(L)], with a higher concentration of puncta in the central domain than in the peripheral regions of the growth cone. However, quantification of myosin V and VI puncta in the peripheral domain, where individual puncta can be better resolved, revealed a 48% reduction of single-labeled myosin V puncta (33 $\pm$ 6 versus control 64 $\pm$ 9 puncta; *t*-test, $p < .01$) and a 71% reduction of single-labeled myosin VI puncta (19 $\pm$ 5 versus control 65 $\pm$ 17 puncta; *t*-test, $p < .01$) when compared with control conditions [Fig. 5(B)]. Double immuno-

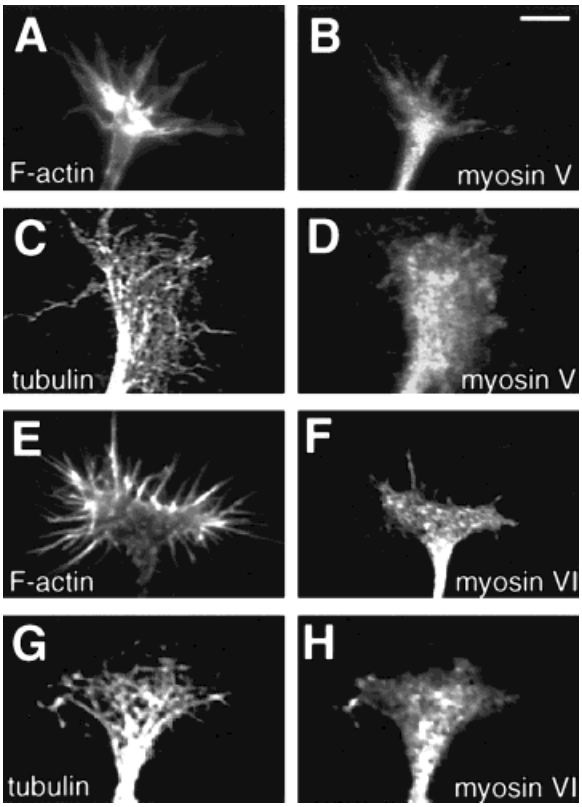

Figure 3 Localization of myosin V and myosin VI with respect to the cytoskeleton in the growth cone. DRG growth cones were double stained for myosin V (B, D; rabbit anti-myosin V head antibody) or myosin VI (F, H; rabbit anti-myosin VI tail antibody) together with F-actin (A, E; rhodamine-phalloidin) or tubulin (C, G; monoclonal antibody), respectively. In the central domain of the growth cone, both myosins are present in the same subcellular region as microtubules. Less myosin V and VI puncta are detected in F-actin–rich filopodia and lamellipodia. Bar: 5 μm.

staining for myosin V and myosin VI after live cell extraction revealed a partial colocalization of these myosins in the growth cone [Fig. 4(H,I,K)] as shown under normal staining conditions [Fig. 4(L)]. Interestingly, double-labeled puncta in the peripheral domain were more resistant to saponin extraction than single-labeled puncta and were reduced only by 30% [9 $\pm$ 2 versus control 13 $\pm$ 2 puncta; *t*-test, $p > .01$; Fig. 5(B)]. These differences in extractability between single- and double-labeled puncta, especially in the case of myosin VI, result in a relative increase of myosin VI in double-labeled puncta after live cell extraction [Fig. 5(A); 34 $\pm$ 5% versus control 18 $\pm$ 3% of total myosin VI in double-labeled puncta; *t*-test, $p < .01$]. Taken together these experiments suggest that a significant portion of both myosin V and myosin VI in the central domain appear to be in relatively tight association with either cytoskeletal or organelle structures. In the peripheral domain, myosin V has a higher association than myosin VI to such structures.

We further investigated and quantified the proportion of soluble myosin V and VI in total embryonic (E10) chick brains as well as in growth cone particles isolated from these brains (Fig. 6). Total brains were homogenized and fractionated by differential centrifugation using the same buffer as in the live cell extraction experiment [Fig. 6(A)]. The amounts of myosin V and VI in each fraction were then analyzed by quantitative Western blotting. The fractionation profile of these two myosins is different after the ultra-high-speed centrifugation step. In agreement with previous findings using 1-day-old brain tissue and different homogenization conditions (Cheney et al., 1993; Evans et al., 1998) the majority of myosin V is found in the 120,000 $\times$ *g* sedimentable fraction containing small organelles [Fig. 6(A); USP]. In contrast, only 37% of the myosin VI was sedimentable at 120,000 $\times$ *g*, whereas 63% remain cytosolic [Fig. 6(A); USS]. These results suggest that in total brain a significant amount of myosin VI is not associated with sedimentable structures such as cytoskeletal filaments and/or organelles.

To better compare the biochemical data with the immunofluorescence growth cone data after live cell extraction, we isolated growth cone particles from embryonic (E10) chick brains according to Pfenninger et al. (1983). Both myosin V and VI can be detected in this growth cone particle preparation; however, they are not enriched when compared with the homogenate [Fig. 6(B)]. In contrast, we found enrichment of GAP-43, which we used as a marker protein for our growth cone particle preparation. As a second control for our growth cone particle isolation, we visualized the particles by high-resolution DIC optics (data not shown). The majority of the particles had a diameter of 0.5–1.5 μm, which is in agreement with their original characterization (Pfenninger et al., 1983). Myosin VI can be saponin-extracted from the growth cone particles to 42% [Fig. 6(B)], whereas extracted myosin V can only be detected after long blot exposures (1–3 min; data not shown). To summarize, myosin VI is more readily extractable than myosin V from growth cone particles as well as from total brain, suggesting a difference in their association state with subcellular structures.

Both unconventional myosins are highly concentrated in the central domain of the growth cones where microtubules are the major cytoskeletal structures (Fig. 3). To investigate a potential association of myosin V and myosin VI with microtubules, we treated the neuronal cultures with the microtubule-

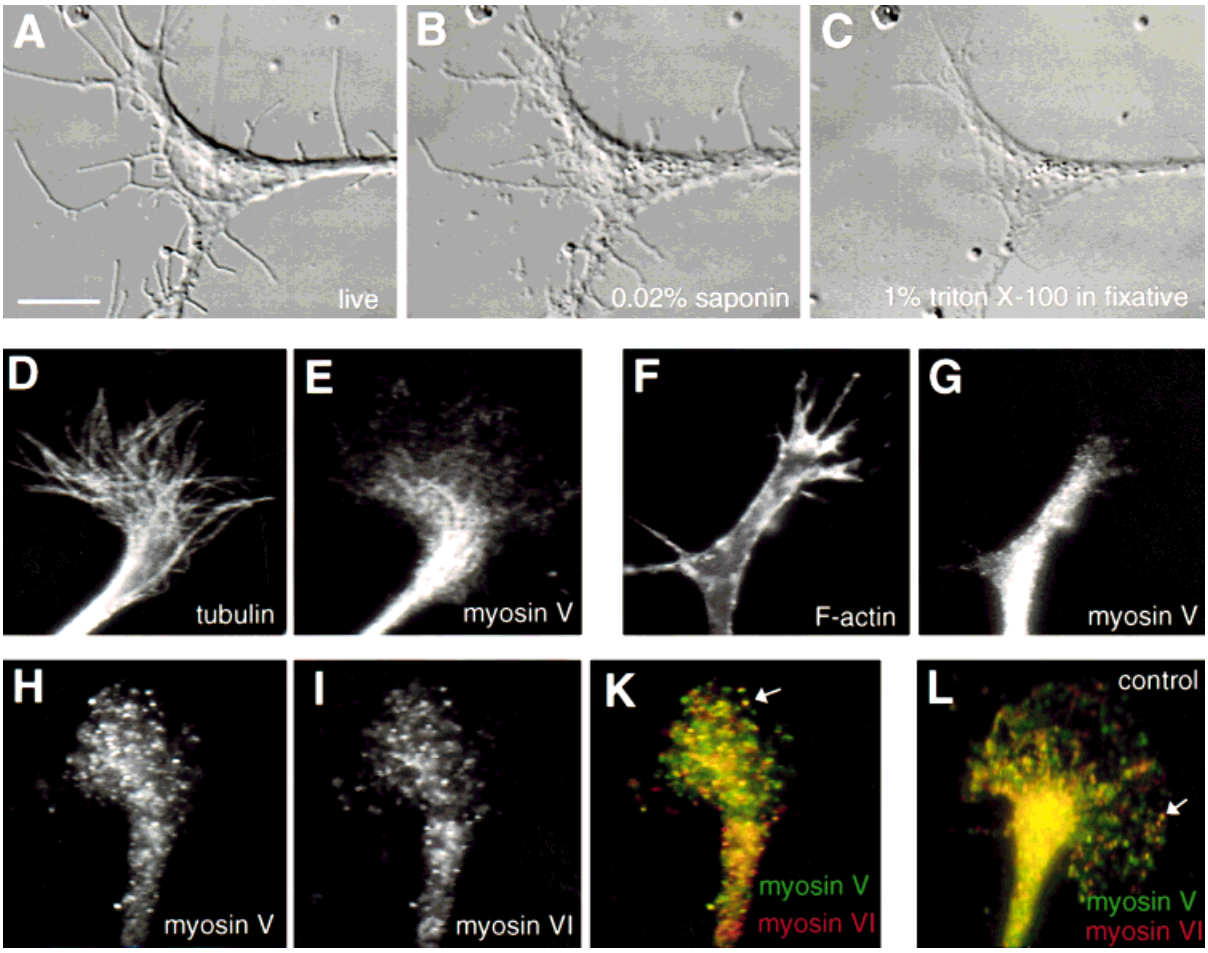

Figure 4 Myosin V and myosin VI puncta in the central domain are resistant to live cell extraction. (A–C) Video-enhanced DIC images showing a DRG growth cone on laminin substrata during the process of a live cell extraction experiment. (A) Live in culture medium. (B) After a 30-s treatment with 0.02% saponin in PHEM buffer. (C) After fixation in the presence of 1% Triton X-100. (D–K) Immunolocalization of myosin V (E and G, rabbit anti-myosin V head antibody; H, rat anti-myosin V head antibody) together with tubulin (D), F-actin (F), and myosin VI (I, rabbit anti-myosin VI tail antibody) reveals that the punctate staining pattern of both myosins remains in the central domain after live cell extraction. (K) Pseudocolor overlay of the myosin V (green) and myosin VI (red) double staining showed in (H) and (I), respectively. Some of the puncta are colocalized (arrow). (L) Pseudocolor overlay of myosin V (green) and myosin VI (red) double staining using normal fixation protocol (no live cell extraction) reveals only partial colocalization of myosin V and myosin VI puncta in the peripheral domain (arrow). Bar: 5 μm.

depolymerizing drug nocodazole (1 μM) for 1 h (Fig. 7). Such treatment resulted in disruption of microtubule structures in the central and peripheral domain of the growth cone [Fig. 7(C,E)] compared to control growth cones [Fig. 7(A)], whereas higher doses of nocodazole had more severe effects on growth cone morphology, making myosin V and VI localization difficult. The effect of the nocodazole treatment also is demonstrated by the diffuse tubulin immunofluorescence staining pattern in both lamellipodia and filopodia [Fig. 7(C,E)], suggesting higher levels of free tubulin relative to control growth cones [Fig. 7(A)]. However, disruption of microtubules in the growth cones did not appear to affect myosin V or myosin VI localization significantly [Fig. 7(D,F)]. Interestingly, nocodazole-treated growth cones had longer filopodia than control growth cones containing both myosin V and VI puncta. To summarize, the results of the nocodazole experiments suggest that distribution of these myosins within the growth cone does not require direct interaction with microtubules.

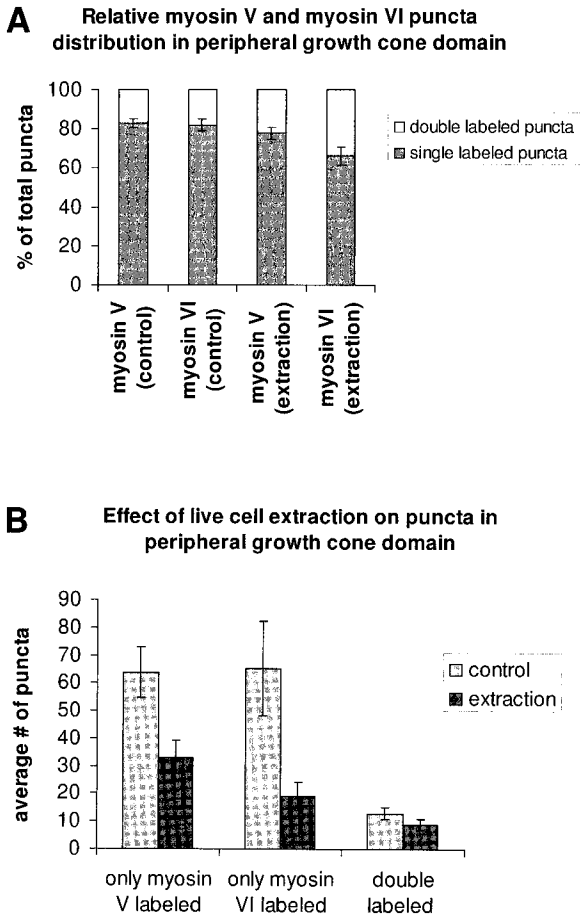

Figure 5 Quantification of myosin V and myosin VI puncta in peripheral growth cone domains. Single- and double-labeled myosin V and VI puncta were counted in the peripheral domain of growth cones under control ($n = 6$) and live cell extraction condition ($n = 5$; see Methods; average values ± S.E.M. are given). (A) Relative puncta distribution of single- and double-labeled puncta for each myosin. Note: increase in the relative fraction of myosin VI label in double-labeled puncta after live cell extraction. (B) Reduction of the number of myosin V and VI puncta in the peripheral growth cone domain after live cell extraction.

DISCUSSION

Localization of Myosin V and Myosin VI in Growth Cones

In this study, we found that both myosin V and myosin VI are highly expressed in the chicken brain and DRGs during embryonic development. Our myosin V data are in agreement with previous studies on myosin V expression (Mercer et al., 1991; Espindola et al., 1992; Espreafico et al., 1992). In contrast, the expression pattern of myosin VI has not been well characterized to date. With respect to the nervous system, myosin VI has been localized in the sensory hair cells of the inner ear (Avraham et al., 1995; Hasson et al., 1997), and very recently the *Drosophila* myosin VI homologue, 95F, has been detected in axons of the central nervous system in fly embryos (Lantz and Miller, 1998).

In the growth cone, both myosin V and myosin VI exhibit a punctate staining pattern that is concentrated in the central domain. Here, both myosins are present in the same subcellular region as microtubules. The punctate staining patterns suggest that both myosins

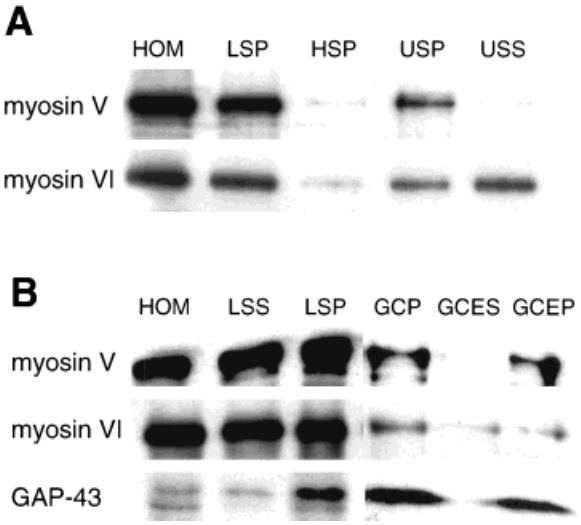

Figure 6 Myosin V and myosin VI are differentially associated with growth cone particles. (A) Myosin V and VI from embryonic brain exhibit different fractionation patterns. Whole brains from chick embryos (E10) were homogenized and fractionated by differential sedimentation (see Methods). Stochiometric samples from each fractionation step were separated on 5–20% SDS-PAGE and included the whole brain homogenate (HOM), the low- (LSP), high- (HSP) and ultra- (USP) speed pellets as well as the ultra-speed supernatant (USS). Western blots were probed with rabbit anti-myosin V tail (top row) and rabbit anti-myosin VI tail antibody (bottom row), respectively. A major difference between myosin V and myosin VI was detected in ultra speed centrifugation step: myosin V is found predominantly in the pellet fraction (USP), whereas a higher fraction of myosin VI is found in the supernatant (USS). (B) Myosin V and VI are differentially extracted from growth cone particle preparations. Growth cone particles were isolated from whole embryonic chick brains (E10; see Methods). Equal protein amounts from each fractionation step were separated on 5–20% SDS-PAGE and included the following samples: homogenate (HOM), low-speed supernatant (LSS) and pellet (LSP), growth cone particles (GCP), supernatant (GCES), and pellet (GCEP) after saponin extraction of growth cone particles. Western blots were probed with rabbit anti-myosin V tail, rabbit anti-myosin VI tail and mouse anti-GAP-43 antibody, respectively. Myosin V and VI are present, but not enriched in growth cone particles.

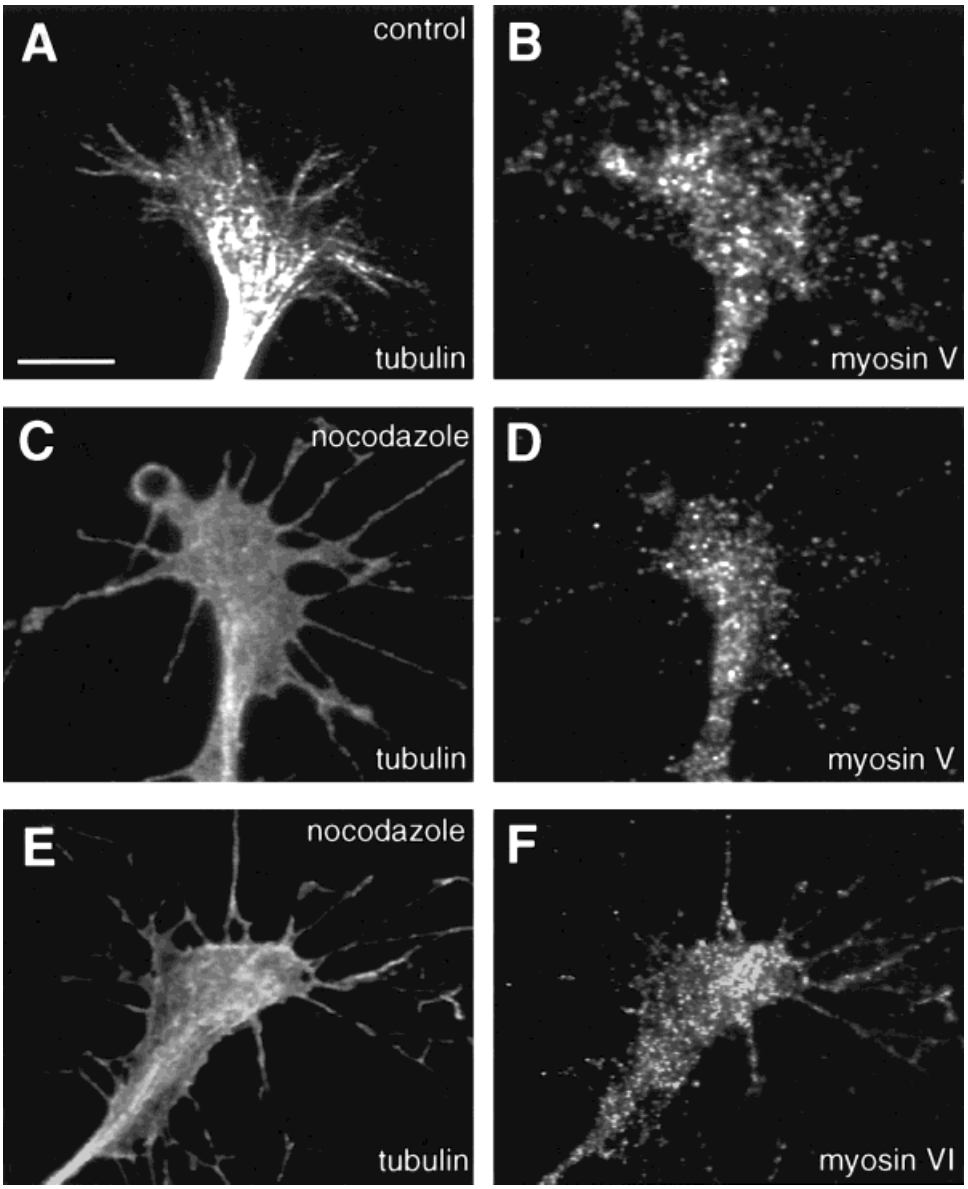

Figure 7 The punctate distributions of myosin V and VI within the growth cone are not altered by the disruption of microtubules. DRG growth cones cultured under control conditions (A, B) and after treatment with 1 μM nocodazole for 1 h (C–F) were double stained for tubulin (A, C, E) and myosin V (B, D) and myosin VI (F). Nocodazole treatment caused a disruption of microtubule structures within the growth cone (C, E), but did not change the punctate myosin V (D) and myosin VI (F) distribution significantly. Bar: 5 μm.

may be associated with vesicular structures; however, this may not be true for all puncta, as recently demonstrated in other myosin localization studies (Lewis and Bridgman, 1996; Evans et al., 1997). Our findings on myosin V distribution in growth cones of cultured chick DRG neurons is in complete agreement with the results of a recent study on myosin V localization in growth cones of rodent superior cervical ganglia neurons (Evans et al., 1997). Evans et al. detected myosin V immunogold-labeling on organelles that are associated with microtubules. However, a direct microtubule association was not found, which is in agreement with the result of the nocodazole experiment in our study as well as that done by Evans et al. (1997).

This study is the first to show localization of a class VI myosin in growth cones. The presence of myosin VI in the microtubule-rich central domain is important to note, since it was recently found that *Drosophila*

myosin VI coimmunoprecipitates with a microtubule-binding protein D-CLIP-190 (Lantz and Miller, 1998). Although myosin VI exhibits a similar punctate distribution in the growth cone as myosin V, we found only partial colocalization in the peripheral domain (18% of all myosin VI puncta in double-labeled puncta), suggesting that a significant portion of these myosins may be associated with distinct vesicular or cytoskeletal structures. In addition, the live cell extraction experiments revealed that these myosins differ in their association state at least in the peripheral domain, where individual puncta can be analyzed. The higher extractability of myosin VI puncta from the peripheral domain (Fig. 5) is in agreement with the results of our biochemical fractionation of total brain tissue as well as of our growth cone particle preparation (Fig. 6). These results indicate that a larger fraction of myosin VI than of myosin V in total brain tissue and growth cones is cytosolic and/or only weakly associated with cytoskeletal/organelle structures. Differences in the levels of extractability, when comparing the three methods for the same myosin, could be explained both by the different starting material used for quantification (peripheral domain of cultured growth cones, total brain, growth cone particles), and by the different technical approaches. To summarize, all of our results suggest that a major fraction of both myosin V and VI have distinct subcellular distributions in growth cones.

With which organelles are these myosin motors associated? Two sets of biochemical studies indicate that myosin V is in part associated with membranes containing synaptic vesicle proteins (Prekeris and Terrian, 1997; Evans et al., 1998). Myosin V is present in preparations of synaptic vesicles and can be biochemically crosslinked to the synaptic vesicle proteins, synaptobrevin II and synaptophysin (Prekeris and Terrian, 1997). However, immuno–electron microscopic analysis revealed that the majority of vesicles containing both myosin V and the synaptic vesicle protein, SV2, are much larger (30–250 nm) than mature synaptic vesicles (50 nm), which mostly lack myosin V (Evans et al., 1998). Thus, myosin V may be associated with organelles involved in synaptic vesicle maturation or recycling (Evans et al., 1998). Consistent with the fractionation results of the present study, myosin VI is not enriched in the myosin V/synaptic vesicle–enriched membrane fractions described by Evans et al. (1998; L. Evans and M. Mooseker, unpublished observations).

Functions of Myosin V and Myosin VI in Growth Cones

Myosins of four different classes have been identified in growth cones so far: I, II, V, and VI. Considering the growing myosin superfamily, it is quite possible that myosins of other classes might be localized in this highly specialized neuronal structure. Why are there so many different myosin motors in growth cones and in cells in general? It has become evident that myosins are involved in a variety of cellular functions, such as cell movement, membrane traffic, and signal transduction in different systems (for reviews, see Titus, 1997; Mermall et al., 1998). There is biochemical, genetic, immunocytological, and physiological evidence, suggesting that myosin II and probably myosin I are involved in growth cone motility, whereas myosin V may play a role in organelle transport (reviewed in Hasson and Mooseker, 1997).

Is myosin V just a passenger or actively involved in organelle movement in growth cones? Recent functional studies on brain vesicle–associated myosin V revealed that these organelles are capable of actin-based transport that can be blocked by antibodies against the myosin V motor domain (Evans et al., 1998). A potential role for myosin V in membrane delivery could explain the effects on filopodial dynamics when myosin V protein is locally inactivated in growth cones (Wang et al., 1996). The idea of a myosin acting as an organelle motor in neurons is particularly intriguing since there have been several reports on actin-based organelle transport in the past (Kuznetsov et al., 1992; Bearer et al., 1993; Langford et al., 1994; Evans and Bridgman, 1995; Morris and Hollenbeck, 1995; Evans et al., 1998; Tabb et al., 1998). Thus, there is an interesting possibility that organelles are transported along microtubule tracks by action of kinesin and dynein motors inside the axon, but when they arrive in the growth cone peripheral domain, they switch the transport machinery to the actin/myosin system to achieve their final destination. The recent findings on the direct interaction between myosin Va and kinesin provide further evidence for the functional cooperation of these two motor systems (Huang et al., 1999).

The punctate staining pattern of myosin VI is similar to the one of myosin V, suggesting that myosin VI may also be associated with organelles in the growth cone. There is evidence that myosin VI might be an organelle motor in *Drosophila* embryos and might be involved in cytoplasmic transport during oocyte maturation (Mermall et al., 1994; Mermall and Miller, 1995; Bohrmann, 1997; Lantz and Miller, 1998). However, the function of myosin VI as an organelle

motor needs to be further analyzed, perhaps with an *in vitro* motility assay similar to the one used for myosin V (Evans et al., 1998). Obtaining more information on myosin VI function will help our understanding of why there are so many different myosins in neurons.

The authors thank Lisa Evans for assistance in the cell fractionation studies and helpful comments on the manuscript.

REFERENCES

Avraham KB, Hasson T, Steel KP, Kingsley DM, Russell LB, Mooseker MS, Copeland NG, Jenkins NA. 1995. The mouse Snell's waltzer deafness gene encodes an unconventional myosin required for structural integrity of inner ear hair cells. Nat Genet 11:369–375.

Avraham KB, Hasson T, Sobe T, Balsara B, Testa JR, Skvorak AB, Morton CC, Copeland NG, Jenkins NA. 1997. Characterization of unconventional MYO6, the human homologue of the gene responsible for deafness in Snell's waltzer mice. Hum Mol Genet 6:1225–1231.

Bearer EL, DeGiorgis JA, Bodner RA, Kao AW, Reese TS. 1993. Evidence for myosin motors on organelles in squid axoplasm. Proc Natl Acad Sci USA 90:11252–11256.

Bement WM, Hasson T, Wirth JA, Cheney RE, Mooseker MS. 1994. Identification and overlapping expression of multiple unconventional myosin genes in vertebrate cell types. Proc Natl Acad Sci USA 91:6549–6553.

Benashski SE, Harrison A, Patel-King RS, King SM. 1997. Dimerization of the highly conserved light chain shared by dynein and myosin V. J Biol Chem 272:20929–20935.

Bohrmann J. 1997. Drosophila unconventional myosin VI is involved in intra- and intercellular transport during oogenesis. Cell Mol Life Sci 53:652–662.

Bunn RC, Jensen MA, Reed BC. 1999. Protein interactions with the glucose transporter binding protein GLUT1CBP that provide a link between GLUT1 and the cytoskeleton. Mol Biol Cell 10:819–832.

Buss F, Kendrick-Jones J, Lionne C, Knight AE, Cote GP, Luzio JP. 1998. The localization of myosin VI at the golgi complex and leading edge of fibroblasts and its phosphorylation and recruitment into membrane ruffles of A431 cells after growth factor stimulation. J Cell Biol 143:1535–1545.

Cheney RE, O'Shea MK, Heuser JE, Coelho MV, Wolenski JS, Espreafico EM, Forscher P, Larson RE, Mooseker MS. 1993. Brain myosin-V is a two-headed unconventional myosin with motor activity. Cell 75:13–23.

Costa MCR, Mani F, Santoro W, Espreafico EM, Larson RE. 1999. Brain myosin-V, a calmodulin-carrying myosin, binds to calmodulin-dependent protein kinase II and activates its kinase activity. J Biol Chem 274:15811–15819.

Espindola FS, Espreafico EM, Coelho MV, Martins AR, Costa FR, Mooseker MS, Larson RE. 1992. Biochemical and immunological characterization of p190-calmodulin complex from vertebrate brain: a novel calmodulin-binding myosin. J Cell Biol 118:359–368.

Espreafico EM, Cheney RE, Matteoli M, Nascimento AA, De Camilli PV, Larson RE, Mooseker MS. 1992. Primary structure and cellular localization of chicken brain myosin-V (p190), an unconventional myosin with calmodulin light chains. J Cell Biol 119:1541–1557.

Evans LL, Bridgman PC. 1995. Particles move along actin filament bundles in nerve growth cones. Proc Natl Acad Sci USA 92:10954–10958.

Evans LL, Hammer J, Bridgman PC. 1997. Subcellular localization of myosin V in nerve growth cones and outgrowth from dilute-lethal neurons. J Cell Sci 110: 439–449.

Evans LL, Lee AJ, Bridgman PC, Mooseker MS. 1998. Vesicle-associated brain myosin-V can be activated to catalyze actin-based transport. J Cell Sci 111:2055–2066.

Forscher P, Smith SJ. 1988. Actions of cytochalasins on the organization of actin filaments and microtubules in a neuronal growth cone. J Cell Biol 107:1505–1516.

Hasson T, Mooseker MS. 1994. Porcine myosin-VI: characterization of a new mammalian unconventional myosin. J Cell Biol 127:425–440.

Hasson T, Skowron JF, Gilbert DJ, Avraham KB, Perry WL, Bement WM, Anderson BL, Sherr EH, Chen ZY, Greene LA, Ward DC, Corey DP, Mooseker MS, Copeland NG, Jenkins NA. 1996. Mapping of unconventional myosins in mouse and human. Genomics 36:431–439.

Hasson T, Gillespie PG, Garcia JA, MacDonald RB, Zhao Y, Yee AG, Mooseker MS, Corey DP. 1997. Unconventional myosins in inner-ear sensory epithelia. J Cell Biol 137:1287–1307.

Hasson T, Mooseker MS. 1997. The growing family of myosin motors and their role in neurons and sensory cells. Curr Opin Neurobiol 7:615–623.

Huang J-D, Brady ST, Richards BW, Stenoien D, Resau JH, Copeland NG, Jenkins NA. 1999. Direct interaction of microtubule- and actin-based transport motors. Nature 397:267–270.

Kellerman KA, Miller KG. 1992. An unconventional myosin heavy chain gene from *Drosophila melanogaster*. J Cell Biol 119:823–834.

Kuznetsov SA, Langford GM, Weiss DG. 1992. Actin-dependent organelle movement in squid axoplasm. Nature 356:722–725.

Langford GM, Kuznetsov SA, Johnson D, Cohen DL, Weiss DG. 1994. Movement of axoplasmic organelles on actin filaments assembled on acrosomal processes: evidence for a barbed-end-directed organelle motor. J Cell Sci 107:2291–2298.

Lantz VA, Miller KG. 1998. A class VI unconventional myosin is associated with a homologue of a microtubule-binding protein, cytoplasmic linker protein-170, in neurons and at the posterior pole of *Drosophila* embryos. J Cell Biol 140:897–910.

Lewis AK, Bridgman PC. 1996. Mammalian myosin I alpha

is concentrated near the plasma membrane in nerve growth cones. Cell Motil Cytoskel 33:130–150.

Lohse K, Helmke SM, Wood MR, Quiroga S, de la Houssaye BA, Miller VE, Negre-Aminou P, Pfenninger KH. 1996. Axonal origin and purity of growth cones isolated from fetal rat brain. Dev Brain Res 96:83–96.

Mercer JA, Seperack PK, Strobel MC, Copeland NG, Jenkins NA. 1991. Novel myosin heavy chain encoded by murine dilute coat colour locus. Nature 349:709–713.

Mermall V, McNally JG, Miller KG. 1994. Transport of cytoplasmic particles catalysed by an unconventional myosin in living *Drosophila* embryos. Nature 369:560–562.

Mermall V, Miller KG. 1995. The 95F unconventional myosin is required for proper organization of the *Drosophila* syncytial blastoderm. J Cell Biol 129:1575–1588.

Mermall V, Post PL, Mooseker MS. 1998. Unconventional myosins in cell movement, membrane traffic, and signal transduction. Science 279:527–533.

Mooseker MS, Cheney RE. 1995. Unconventional myosins. Annu Rev Cell Dev Biol 11:633–675.

Morris RL, Hollenbeck PJ. 1995. Axonal transport of mitochondria along microtubules and F-actin in living vertebrate neurons. J Cell Biol 131:1315–1326.

Nascimento AAC, Cheney RE, Tauhata SBF, Larson RE, Mooseker MS. 1996. Enzymatic characterization and functional domain mapping of brain myosin-V. J Biol Chem 271:17561–17569.

Nascimento AA, Amaral RG, Bizario JC, Larson RE, Espreafico EM. 1997. Subcellular localization of myosin-V in the B16 melanoma cells, a wild-type cell line for the dilute gene. Mol Biol Cell 8:1971–1988.

Pfenninger KH, Ellis L, Johnson MP, Friedman LB, Somlo S. 1983. Nerve growth cones isolated from fetal rat brain: subcellular fractionation and characterization. Cell 35: 573–584.

Prekeris R, Terrian DM. 1997. Brain myosin V is a synaptic vesicle-associated motor protein: evidence for a Ca^{2+}-dependent interaction with the synaptobrevin-synaptophysin complex. J Cell Biol 137:1589–1601.

Probst FJ, Fridell RA, Raphael Y, Saunders TL, Wang A, Liang Y, Morell RJ, Touchman JW, Lyons RH, Noben-Trauth K, Friedman TB, Camper SA. 1998. Correction of deafness in shaker-2 mice by an unconventional myosin in a BAC transgene. Science 280:1444–1447.

Provance DW, Jr, Wei M, Ipe V, Mercer JA. 1996. Cultured melanocytes from dilute mutant mice exhibit dendritic morphology and altered melanosome distribution. Proc Natl Acad Sci USA 93:14554–14558.

Rogers SL, Gelfand VI. 1998. Myosin cooperates with microtubule motors during organelle transport in melanophores. Curr Biol 8:161–164.

Suter DM, Errante LD, Belotserkovsky V, Forscher P. 1998. The Ig superfamily cell adhesion molecule, apCAM, mediates growth cone steering by substrate-cytoskeletal coupling. J Cell Biol 141:227–240.

Tabb JS, Molyneaux BJ, Cohen DL, Kuznetsov SA, Langford GM. 1998. Transport of ER vesicles on actin filaments in neurons by myosin V. J Cell Sci 111:3221–3234.

Takagishi Y, Oda S, Hayasaka S, Dekker-Ohno K, Shikata T, Inouye M, Yamamura H. 1996. The dilute-lethal (dl) gene attacks a Ca^{2+} store in the dendritic spine of Purkinje cells in mice. Neurosci Lett 215: 169–172.

Titus MA. 1997. Motor proteins: myosin V—the multipurpose transport motor. Curr Biol 7:R301–304.

Wang A, Liang Y, Fridell RA, Probst FJ, Wilcox ER, Touchman JW, Morton CC, Morell RJ, Noben-Trauth K, Camper SA, Friedman TB. 1998. Association of unconventional myosin MYO15 mutations with human nonsyndromic deafness DFNB3. Science 280:1447–1451.

Wang FS, Wolenski JS, Cheney RE, Mooseker MS, Jay DG. 1996. Function of myosin-V in filopodial extension of neuronal growth cones. Science 273:660–663.

Wu X, Bowers B, Wei Q, Kocher B, Hammer JA, 3rd. 1997. Myosin V associates with melanosomes in mouse melanocytes: evidence that myosin V is an organelle motor. J Cell Sci 110:847–859.

Wu X, Bowers B, Rao K, Wei Q, Hammer JA. 1998. Visualization of melanosome dynamics within wild-type and dilute melanocytes suggests a paradigm for myosin V function in vivo. J Cell Biol 143:1899–1918.

Zhao LP, Koslovsky JS, Reinhard J, Bahler M, Witt AE, Provance DW, Jr, Mercer JA. 1996. Cloning and characterization of myr 6, an unconventional myosin of the dilute/myosin-V family. Proc Natl Acad Sci USA 93: 10826–10831.